# A Novel Directional Intermittent Ground Fault Detection Method for Compensated Grounded Systems

Henrik Sundholm
*Proelektro Engineering*

Anushka M. Dissanayake, Anirudhh Ravi, Osama Ansari, Vinod Yedidi, and Zafer Korkmaz
*Schweitzer Engineering Laboratories, Inc.*

Revised edition released October 2025

Originally presented at the
52nd Annual Western Protective Relay Conference, October 2025

# A Novel Directional Intermittent Ground Fault Detection Method for Compensated Grounded Systems

Henrik Sundholm, *Proelektro Engineering*
Anushka M. Dissanayake, Anirudhh Ravi, Osama Ansari, Vinod Yedidi, and Zafer Korkmaz,
*Schweitzer Engineering Laboratories, Inc.*

***Abstract*—Compensated networks, grounded through reactors tuned to system capacitance, offer benefits—such as arc suppression, improved power quality, and wildfire mitigation—for electric utilities, and industrial operators seeking enhanced safety, reliability, and environmental resilience. However, compensated networks complicate ground fault detection, particularly for intermittent ground faults (IGFs), which are common in cable networks. IGFs arise from insulation defects, moisture penetration into the cable, cable splices, or impurities within the cable and insulation materials, leading to arcs that self-extinguish at current zero-crossings and reignite due to weakened insulation. These restriking arcs can escalate into permanent faults, and their transient nature makes traditional phasor-based directional detection methods unreliable. Existing IGF detection techniques—based on zero-sequence voltage (V0) and current (I0) polarity, multifrequency admittance, or instantaneous energy—are computationally demanding and require high sampling rates. In this paper, we propose a simpler, more efficient method that uses raw I0 samples and the change of V0 (dV0) to detect IGFs and their direction more quickly and reliably than traditional methods. IGFs are detected by comparing the current dV0 to its recent values, while fault direction is determined by the polarity relationship between dV0 and I0. Our proposed method avoids complex algorithms like Fourier or Hilbert transforms, offering faster detection (under a quarter cycle), enhanced security, and improved dependability. The proposed method can also block unreliable phasor-based directional elements during IGFs. We validate the effectiveness of our method with field data from a compensated distribution system and real-time digital simulator (RTDS) simulations. Our approach is extendable to detect both IGFs and permanent faults in systems using rapid earth-fault current limiter (REFCL) technologies.***

## I. Introduction

As reliance on an uninterrupted electricity supply grows, the demand for quality, safety, and reliability in power delivery also increases. To enhance the quality and availability of electricity and to improve safety measures—such as wildfire mitigation—resonant grounding together with rapid earth-fault current limiter (REFCL) has become a widely adopted method for neutral point grounding in distribution networks outside the North American market. The fault arc suppression nature of compensated networks plays a crucial role in improving power reliability and public safety.

While compensated networks offer advantages, they also complicate ground fault detection and protection. Previous field experiences show that ground faults in compensated networks frequently exhibit a transient nature, especially in cable networks. Such faults may restrike intermittently and are commonly referred to as intermittent ground faults (IGFs). Factors, such as defects and impurities (which may originate during the insulation aging process from chemical reactions or by being introduced during cable manufacturing) or moisture in cable joints, can initiate arcs [1]. Typically, the fault arc self-extinguishes at the natural zero-crossing of the fault current but then reignites due to the reduced dielectric strength of the damaged insulation at the fault location (FL) [1]. These restriking arcs may lead to a breakdown and subsequently to a permanent fault. Given the transient and often low-energy nature of IGFs, traditional phasor-based protection schemes often struggle to provide reliable and timely fault detection.

Commonly identified IGF detection methods identify the presence of IGFs by using the polarity of zero-sequence voltage (V0) and zero-sequence current (I0), or by determining the multifrequency admittance with the cumulative phasor summation (CPS), or by estimating the instantaneous zero-sequence energy [1] [2] [3] [4] [5] [6]. However, the existing methods are computationally intensive and require higher sampling rates of IEDs to be reliable.

In this paper, we present a method that uses raw samples of 3I0 and the change of V0 (dV0) to determine the IGF direction. The logic we propose compares the present dV0 to a series of most recent dV0s to detect the fault. We determine the direction by comparing the polarity of dV0 and 3I0. Analysis and field events show that polarities of dV0 and 3I0 are the same for a reverse fault and the opposite for a forward fault. We also present the advantages of using dV0 over V0 with respect to security and dependability. Our proposed method is computationally less demanding and simpler compared to the commonly identified existing methods as it does not require complex mathematical algorithms, such as Discrete Fourier Transform (DFT), Hilbert transforms, or higher-frequency admittance calculations in IEDs.

The IGF directional method we propose can detect an arc in less than a quarter of a power system cycle. The element output can be further used to block any phasor-based ground directional elements to enhance security. This idea can be extended and evaluated to detect both permanent faults and IGFs in the networks that use REFCL technologies. We

validated our proposed method using field events captured from a compensated distribution system.

The remainder of the paper is organized as follows. We begin by reviewing existing IGF detection methods. Next, we discuss various grounding schemes, with a focus on compensated grounded systems. We then outline the challenges associated with IGF detection, followed by our proposed detection method. We also present a method to approximate percentage tuning of the Petersen coil. After that, we present both simulated and real-world IGF event results to validate our proposed approach, followed by the conclusion.

## II. Existing IGF Detection Methods

The challenges posed by IGFs in compensated distribution networks drove the development of various fault detection techniques, each with their own strengths and limitations. In this section, we explore several commonly identified IGF detection methods, including those based on multifrequency admittance, CPS, and raw sample analysis. By examining these approaches, we aim to highlight the trade-offs between computational complexity, detection speed, and reliability—setting the stage for our proposed method, which leverages raw 3I0 and dV0 samples for efficient and deterministic fault direction.

The fundamental method described in [1] combines spike detection with a phase angle criterion to enhance protection against IGFs. The spike detection approach identifies residual current spikes of a specific polarity, with respect to the residual voltage, which are characteristic of such faults. To enhance security and reduce the likelihood of false operations, this method incorporates counter logic and a configurable drop-off timer. This timer ensures the protection system does not reset between fault pulses, thereby maintaining system readiness and enabling timely operation.

In conjunction, the phase angle criterion evaluates the angular difference between the residual current and residual voltage phasors. The angular difference is measured from both faulty and healthy feeders. Protection is triggered when this phase angle falls within a predefined operating sector and the signal amplitudes exceed set thresholds. Fault resistance can reduce the available residual current to a small value, which may be hard to measure reliably, leading to angle computation errors. For reliable operation, both methods require higher sampling frequency to record discharge transients accurately. False starts are observed with the phase angle method when the system is heavily over compensated (OC) or under compensated (UC).

The method described in [2] for IGF detection is based on the patented concept of CPS in combination with the multifrequency neutral admittance measurement. The main advantage of monitoring the ratio of I0 and V0 (i.e., the neutral admittance) is that, ideally, the result is not affected by the fault resistance in the fault spot. This is because both the I0 and V0 are decreased with increasing fault resistance value; their ratio remains constant. In addition to measuring the fundamental frequency component, the algorithm also detects and measures the harmonic components when their magnitudes are high enough to ensure reliable measurement.

CPS is a concept where the discrete directional admittance phasors are replaced by the accumulated values of the same quantities during the fault. CPS is the result of adding the values of the computed complex DFT-phasors together in phasor format, starting at fault initiation.

The directional phasor calculated by the CPS technique gives an indication of the fault direction as the accumulated fault phasor points towards the direction of the highest energy flow (i.e., in the direction of the fault). If harmonic components are present, then the directional phasors in the faulty and healthy feeders point in opposite directions.

The Berggren method, described in [3], is a patented technique for detecting IGFs using only phase currents without requiring voltage measurements or core current transformers (CTs). This method consists of three key criteria: 3I0 current presence, incremental current differences (Idelta), and a sample polarity check. The system first identifies ground fault conditions by summing phase currents (IA + IB + IC) and setting a threshold trigger. It then calculates incremental changes in phase currents over 20 ms intervals at a 1 kHz sampling rate, followed by a polarity check to confirm the fault. This method is based on the asymmetry between current changes in the three phases. The asymmetry is considerable at low-resistive ground faults but decreases with increasing fault resistance. The level of sensitivity is therefore limited by continuous load current changes and the accuracy of the measurement.

The algorithm discussed in [4] looks for spikes in I0 and V0 generated by IGFs. This algorithm can remove all unnecessary and confusing data and concentrate only on the spikes. By calculating the delta of raw samples using a patented admittance-based formula, the polarities of the spikes in I0 and V0 are determined to distinguish a faulty feeder from a healthy one. To work effectively, the algorithm requires a more accurate 0.2S class measurement CT (typically used in revenue metering), along with a 3.2 kHz sampling frequency. The reliance on spike-based detection means it could be sensitive to external transient disturbances, potentially leading to false positives in networks with high-switching transients.

Reference [5] presents a method and system for detecting IGFs in three-phase medium-voltage (10 kV–35 kV) electric power distribution systems. This method uses transient direction detection based on instantaneous power analysis and Hilbert transform to determine fault direction, distinguishing faulty lines from healthy ones. Additionally, random intermittent detection tracks intermittent changes in residual current amplitude, counting spikes and adjusting thresholds dynamically. The system classifies faults into intermittent, transient, or noise and provides alarms for maintenance actions, and it is designed for various grounding configurations, including resistor-grounded, Petersen coil-grounded, and isolated neutral systems.

The performance of the method presented in [5] heavily depends on the sampling rate. If the sampling rate is too low, important transient details may be missed. The method relies on

the Hilbert transform and instantaneous power analysis, which both can be affected by noise. This method is designed for transient and intermittent faults but may not effectively detect high-impedance faults with small current magnitudes. The adaptive threshold can lead to false alarms if not properly tuned, potentially misclassifying harmless transient spikes (e.g., switching events) as faults.

Reference [6] presents an advanced method for detecting IGFs in medium-voltage distribution networks. This method improves traditional admittance-based techniques by analyzing V0 and zero-sequence admittance parameters ($Y_0$, $G_0$, and $B_0$), while calculating the cumulative duration of intermittent fault arcing. This method detects faults in compensated, ungrounded, and resistance-grounded networks and uses real-time simulations and field-recorded data to validate its effectiveness. This method requires high sampling frequencies (ranging from 6.4 kHz to 245.75 kHz). And this requirement for higher sample rates demands advanced hardware capable of handling intensive signal processing and decision-making algorithms. Fault detection can be more challenging in the case of a high-resistance fault due to sensitivity limitations. Additionally, proper tuning of the threshold values for admittance and fault duration criteria is required for optimal performance, increasing the complexity of relay settings and implementation in real-world networks.

## III. Distribution System Grounding and Compensated Grounded Systems

System grounding is predominantly performed to limit the voltage to ground of the healthy phases within permissible limits during a ground fault event and to enable detection of unexpected connections to ground caused by ground faults due to vegetation contact, falling conductors, or lightning strikes. By limiting the voltage of healthy phases, the voltage stress on conductor insulation is limited and the effects associated with shock hazards caused by contact with live conductors are reduced. Typically, a system is grounded at one point or at multiple points, and the grounding type is either solidly grounded, impedance grounded, or ungrounded [7]. Ungrounded systems have no intentional ground connection to the system conductors and are effectively grounded through the system phase-to-ground capacitance. These systems offer the advantage of operating during a ground fault due to no change in the phase-to-phase voltages, as seen by the voltage triangles in Fig. 1, before the fault Fig. 1(a), and during a phase-A-to-ground fault Fig. 1(b). However, these systems experience excessive overvoltage during arcing or ground faults, and the detection or location of ground faults gets challenging due to the low ground current magnitude under high-impedance faults.

On the other hand, grounded systems offer the advantages of better safety and the limitation of overvoltage during arcing or ground faults. In solidly grounded systems, the system neutral is directly connected to ground, and to preserve the benefits of grounding—especially the limitation of overvoltage—the effective zero-sequence resistance and reactance of these systems are limited relative to their positive-sequence resistance and reactance.

In resistance-grounded systems, one or more resistors are connected between the system neutral and the ground. Depending on the permissible magnitude of ground fault current, these systems can be classified as low-impedance grounded or high-impedance grounded. If the impedance is purely resistive, low-resistance-grounded systems typically limit ground fault current levels to be within 1 kA; whereas, high-resistance-grounded systems limit ground fault current levels within 10 A [7].

High-impedance grounded systems are designed to enhance both the reliability and safety of power systems. Reliability is improved by allowing continued operation of loads during single-line-to-ground faults. Safety is enhanced by limiting fault current levels. Immediate fault detection and isolation are typically not required in these systems. However, in applications where wildfire risk is a concern, fast detection and isolation of single-line-to-ground faults can be beneficial. This grounding is limited to generators or substation transformers where the ground fault current needs to be limited within the three-phase fault current. Instead of resistive grounding, the system can be resonant grounded, where a reactor that is tuned to the system charging current is connected between the system neutral and the ground. This reactor is referred to as a Petersen coil (named after its inventor) or an arc suppression coil. The system is known as a Petersen coil-grounded system or a compensated grounded system.

Resonant grounded systems have become popular in systems prone to wildfires that are largely caused by vegetation contact with live conductors, due to the fault arc suppression property and low ground fault current magnitude. In resonant grounded systems, the ground fault current is almost purely resistive with low fault current magnitude, which prompts the requirement of a sensitive ground fault detection scheme.

In these systems, at the inception of a ground fault, assuming that it is a bolted fault (i.e., a fault with zero fault impedance), the faulted phase voltage goes to ground potential and the unfaulted phase-to-ground voltages rise to $\sqrt{3}$ times their pre-fault voltage levels, which results in a capacitive current flow in the system, where the capacitances in the unfaulted phases are charged due to the higher voltage level, while the capacitances in the faulted phases are discharged due to the ground potential. The flow of resistive, capacitive, and reactor currents and their phasor relationship, are shown in Fig. 1.

The voltage triangle during a single-line-to-ground fault in these systems can be drawn as illustrated in Fig. 1. In Fig. 1 (b), we can see that the line-to-ground voltage increased by $\sqrt{3}$ times that of the healthy voltages. This voltage relationship results in the rise of the zero-sequence voltage, which becomes useful in detecting ground faults.

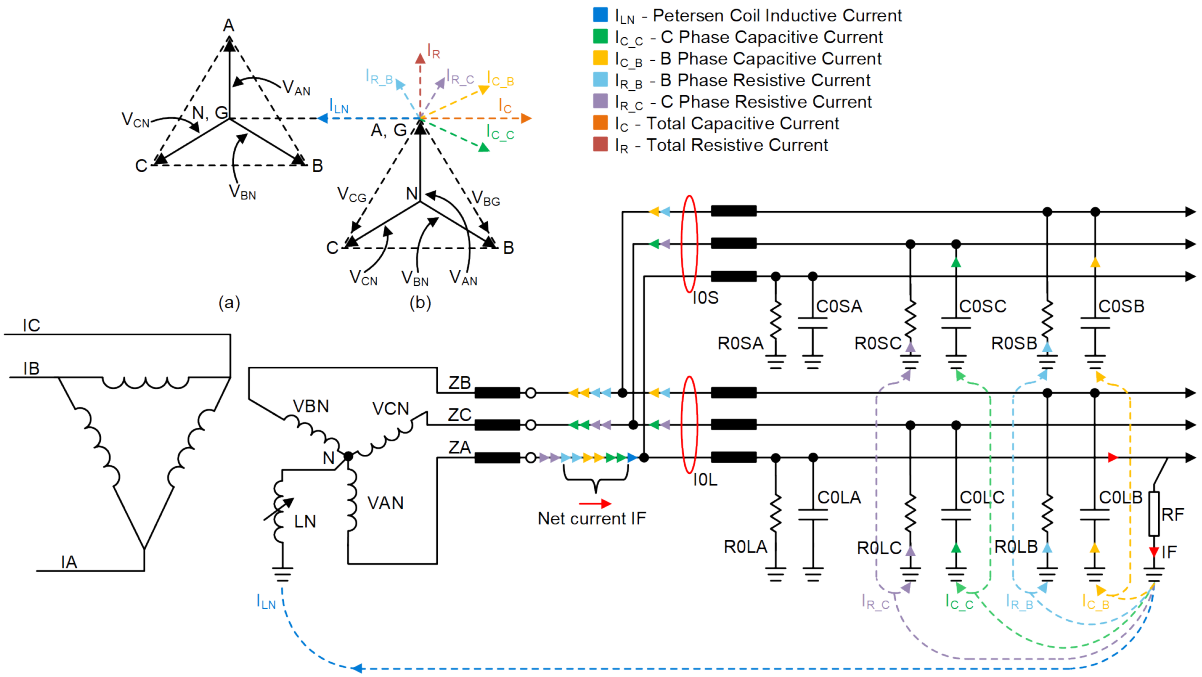


Fig. 1. Overview of a compensated system during a line-to-ground fault (a) voltage triangle before the fault, and (b) during a phase-A-to-ground fault.

As illustrated in Fig. 1, the charge flow is such that the net effective current of the capacitive charging and discharging currents, Petersen coil inductor current and total resistive current from the leakage conductance and active losses, flows through the faulted phase via the ground path. The discharge current flows at higher frequency, typically between 500 and 2,500 Hz, while the charging current typically flows at frequencies in the range of 100–800 Hz [8] [9]. These high-frequency components last for an extremely short time period before going back to the system nominal frequency. In compensated cable systems, the ground faults typically start intermittently due to the self-healing insulation and fault arc suppression, therefore, these faults are termed as IGFs. These faults gradually degrade the insulation, and when the insulation completely degrades, the fault becomes permanent. Therefore, as the ground faults have high-frequency components and can quickly self-extinguish, a fast fault detection scheme is necessary.

## IV. Challenge of Reliable IGF Detection

IGF spikes are short-duration arcs, typically lasting between 1 to 3 milliseconds. A widely used method for determining the direction of an IGF involves comparing the polarity of the zero-sequence voltage sample (V0) and the zero-sequence current sample (I0). For a forward IGF spike, V0 and I0 have opposite polarities, while for a reverse IGF spike, they share the same polarity.

However, this method provides reliable directional information for only a brief period during the initial peak of the transient period, as we demonstrate next. Additionally, a high sampling rate is necessary to accurately capture this initial transient and to ensure this method's reliability.

Zero-sequence voltage and current of a forward IGF in a compensated 50 Hz distribution system (recorded at a 10 kHz sampling rate) are shown in Fig. 2, and a zoomed-in version is shown in Fig. 3. In Fig. 3, two main regions, Region 1 and Region 2, can be identified within the initial spike. Each region lasts approximately 1 ms.

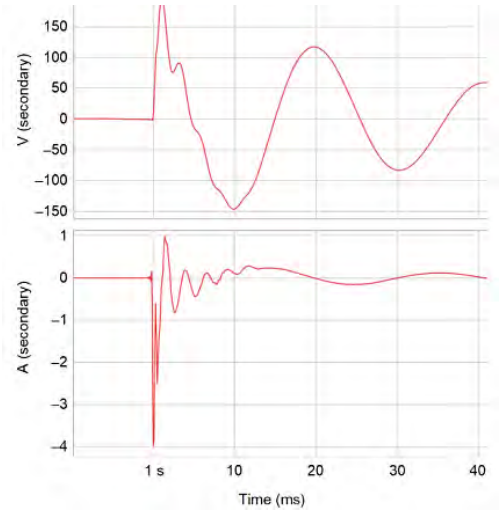


Fig. 2. Zero-sequence voltage (top) and current (bottom) during a forward IGF.

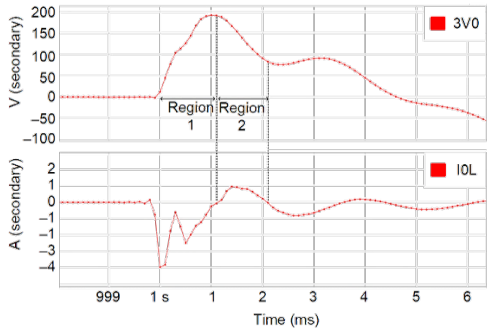


Fig. 3. Zoomed-in version of the initial peak of the zero-sequence voltage (top) and current (bottom) during a forward IGF.

Region 1 contains the critical information needed to determine the direction of the IGF by comparing the polarity of V0 and I0. However, if the protective relay operates at a low sampling rate (e.g., 32 samples per cycle), it becomes challenging to capture enough data points to dependably detect the fault direction. For example, if the relay sampling rate is 32 samples per cycle, only one or two samples may be captured during Region 1, which might not be sufficient to make a reliable decision. Therefore, we need a more reliable method for detecting IGFs than simply comparing the polarity of V0 and I0.

Furthermore, using the polarity comparison of V0 and I0 for determining direction can lead to incorrect results during Region 2, where both signals share the same polarity. As a result, this method may compromise both the dependability and security of the relay when operating at a low sampling rate.

As demonstrated in the following section, more dependable and secure results can be achieved by comparing the polarity of the rate-of-change-of-zero-sequence voltage (dV0/dt) or by change of zero-sequence voltage (dV0) with the zero-sequence current I0.

## V. Proposed IGF Detection Method

### A. Theory and Background

Fig. 4 (a) illustrates a one-line diagram of a compensated radial distribution system, where the relay location defines the protected line. The other distribution lines are combined into an equivalent impedance representing the remaining distribution system. Fig. 4(b) provides an approximate zero-sequence representation of the system. Here, $C_{0L}$ and $R_{0L}$ denote the zero-sequence capacitance and the leakage resistance of the protected line, respectively, while $C_{0S}$ and $R_{0S}$ represent these values for the remainder of the system. In this context, $C_0 = C_{0L} + C_{0S}$ and $1 / R_0 = 1 / R_{0L} + 1 / R_{0S}$, where $C_0$ and $R_0$ are the total system zero-sequence capacitance and leakage resistance, respectively. Parallel equivalents of the Petersen coil series inductance (L) and resistance (R) are shown as $L_N$ and $R_N$ respectively (i.e., $L_N = (R^2 + w^2L^2)w^2$ and $R_N = (R^2 + w^2L^2) / R$) [10].

To represent a fault, we connect an equivalent Thevenin source in series with resistance. Fig. 4(b) shows that closing switch $S_F$ simulates a ground fault on the protected line (forward fault direction from the relay's perspective), while closing Switch $S_R$ simulates a ground fault elsewhere in the system (reverse direction fault).

During a forward single-line-to-ground (SLG) fault, the zero-sequence current seen by the relay ($i_{0L}(t)$) can be written as a function of the Petersen coil current and the current in the remainder of the system, as shown in (1),

$$i_{0L}(t) = -\left( C_{0s}\frac{dv_0(t)}{dt} + \frac{v_0(t)}{R_{0s}} + \frac{1}{3L_N}\int_{t_0}^{t} v_0(t)dt + \frac{v_0(t)}{3R_N} \right) \quad (1)$$

where $v_0(t)$ is the zero-sequence voltage.

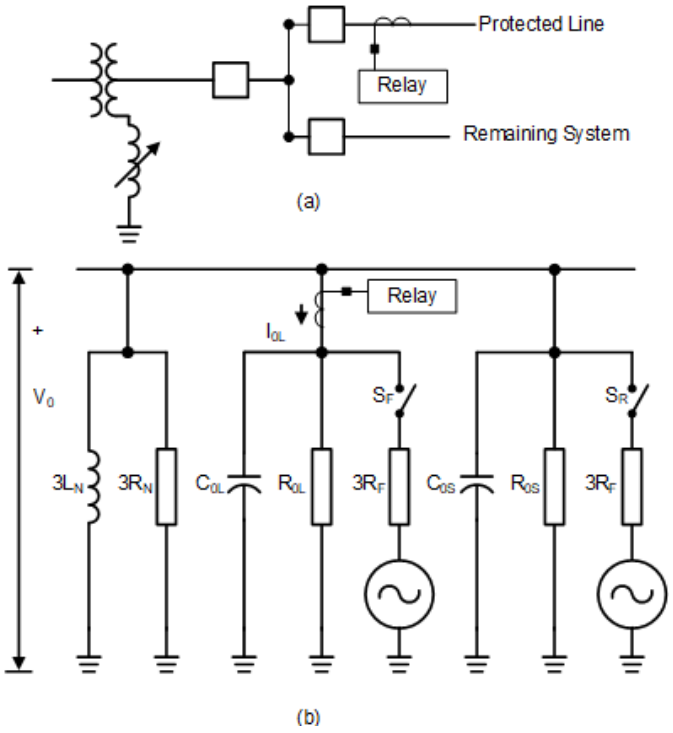


Fig. 4. Compensated grounded system: (a) one-line diagram, (b) zero-sequence network.

The initial zero-sequence transient current primarily consists of the capacitive discharge current of the faulted phase, the capacitive charging currents of the unaffected phases, the Petersen coil inductive charging current, and the resistive currents from the zero-sequence leakage resistance ($R_{0s}$) and the inductor resistance ($3L_N$).

Since the zero-sequence leakage resistance $R_{0s}$ and the inductor resistance $3R_N$ are significantly large, resistive current does not contribute much to the $i_{0L}(t)$ current during the initial transient period.

And because current through an inductor cannot change instantaneously, the Petersen coil inductive charging current does not contribute much to the $i_{0L}(t)$ current during the initial transient period.

The frequency of the initial charging and discharging transient during a fault is much higher than the system nominal frequency. The charge transient frequency usually ranges from 100 Hz to 1,000 Hz [1] [8] [9]. In contrast, the discharge transient frequency is significantly higher, typically 4 to 20 times that of the charge transient [1]. Due to this high frequency, the impedance of the Petersen coil is also high and the inductive current component in (1) is much less compared to the capacitive current. Hence, the capacitive current $C_{0s}$•($dv_0(t) / dt$) dominates the relay measured $i_{0L}(t)$ current in compensated systems during the initial transient.

During a reverse SLG fault, the zero-sequence current seen by the relay ($i_{0L}(t)$) can be written as a shown in (2).

$$i_{0L}(t) = \left( C_{0L}\frac{dv_0(t)}{dt} + \frac{v_0(t)}{R_{0L}} \right) \quad (2)$$

Equations (1) and (2) show that for a forward fault $i_{0L}(t)$ and $dv_0(t)/dt$ are in opposite polarity and for a reverse fault, they are in the same polarity. Therefore, a polarity check between $dv_0(t)/dt$ and $i_{0L}(t)$ can be used to detect the direction of IGFs. Rather than calculating the continuous derivative of $v_0(t)$, similar results can be obtained by using the difference voltage $dv_0(k)$ in a digital relay where $k$ is the sampling index ($dv_0(k) = v_0(k) - v_0(k-1)$ ).

### B. *Forward-Clearing Fault May Appear As a Reverse IGF*

Just after a forward SLG arcing fault (i.e., Switch $S_F$ in Fig. 4 (b) opens) the zero-sequence circuit enters a state of parallel resonance. During the discharge of energy stored in the reactive components of the circuit, the zero-sequence current observed by the relay is the same as described in (2). The signature of this forward-clearing arcing fault is identical to that of a reverse arcing fault. Therefore, additional security measures must be implemented to block the reverse logic if the relay detects any forward activity.

### C. *Event Analysis*

We use the same IGF event, shown in Fig. 3, to validate the theory explained in the previous section. The difference voltage $dv_0$ and the corresponding zero-sequence currents captured by two relays are shown in Fig. 5. The IGF spike is forward to the relay that captures the current $i_{0L}$ and reverse to the relay that captures the current $i_{0S}$.

In both Region 1 and Region 2, $dv_0$ and $i_{0L}$ are in opposite polarity and $dv_0$ and $i_{0S}$ are in the same polarity. Hence, this event analysis proves that the polarity checks between $dv_0$ and $i_0$ quantities can be used to reliably detect the direction of IGF spikes.

### D. *Logic for a Digital Relay*

This section presents a logic that can be implemented in a digital relay to detect IGFs based on the ideas presented in the previous sections.

The proposed method uses raw samples of the measured (or calculated from phase quantities) zero-sequence voltage (3V0) and the measured zero-sequence current (3I0) to detect an IGF and determine its direction. During an IGF, 3V0 increases rapidly; therefore, the occurrence of an IGF is identified by analyzing the change of 3V0 (denoted as dV0). The detection logic compares the current dV0 with a series of recent dV0 values. An IGF is detected if the current dV0 is significantly larger than the previous values. The direction of the fault is determined by comparing the polarity of dV0 and 3I0.

An overview of the logic is shown in Fig. 6. The logic is initiated when the absolute value of the measured zero-sequence voltage sample (abs(3V0)) is greater than a threshold (3V0_thr). Each sublogic is explained in the following sections.

The dV0 calculation logic determines the difference between two consecutive 3V0 samples, as illustrated in Fig. 7. A first-in, first-out circular buffer stores the most recent dV0 values for later referencing.

The polarity check logic compares the polarity of dV0 and 3I0, as shown in Fig. 8. If the polarities are opposite, the forward (FWD) output is set to 1. If they are the same, the reverse (REV)output is set to 1. The thresholds dV0_thr and 3I0_thr can be small positive values. As an alternative method, the product of dV0 • 3I0 can be compared to a small threshold to determine whether the polarities of dV0 and 3I0 are opposite or similar.

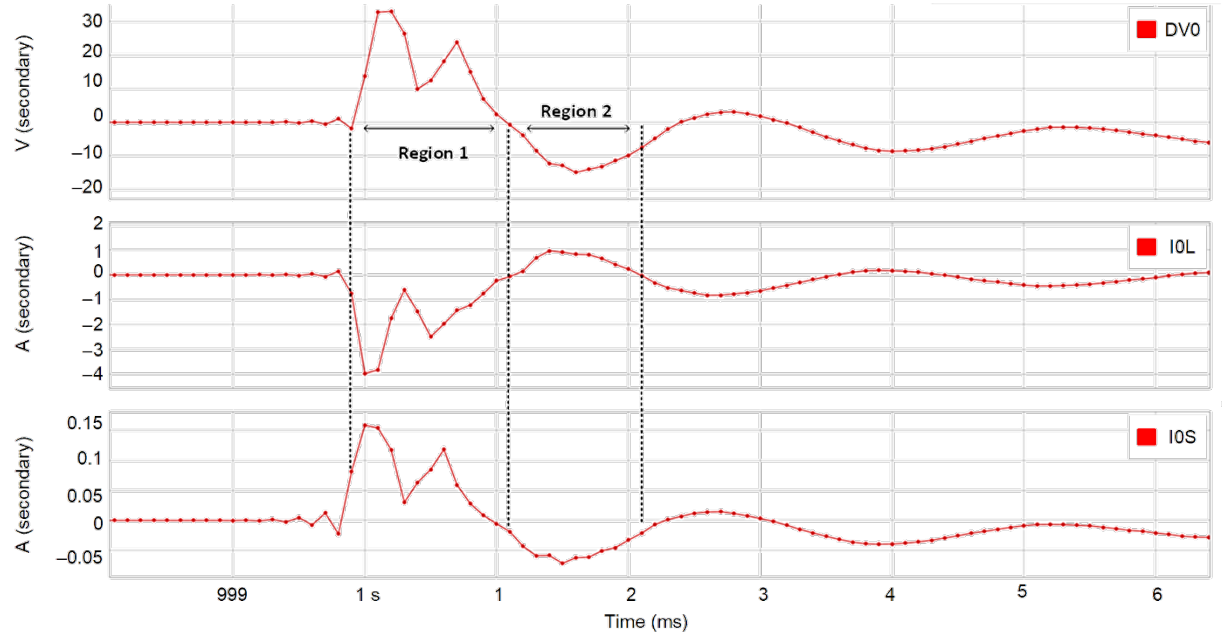


Fig. 5. Zero-sequence difference voltage ($dv_0$) and zero-sequence currents during an IGF spike.

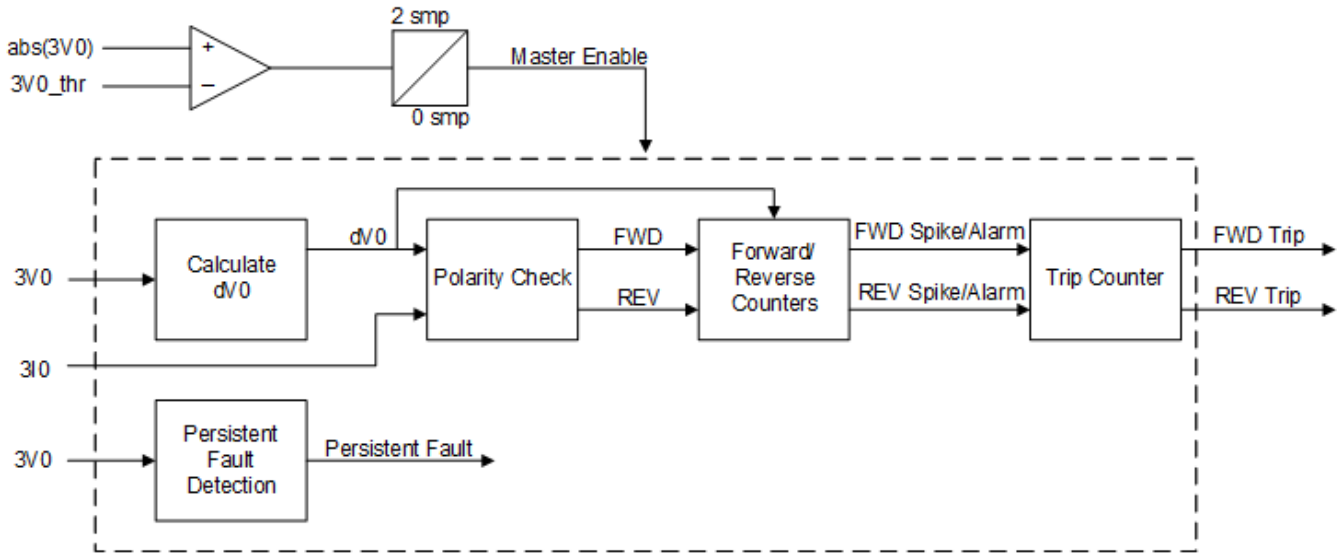


Fig. 6. Overview of the logic.

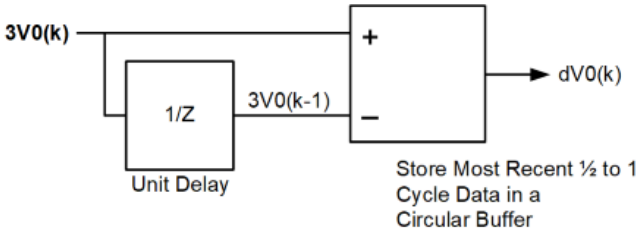


Fig. 7. Calculate dV0 logic.

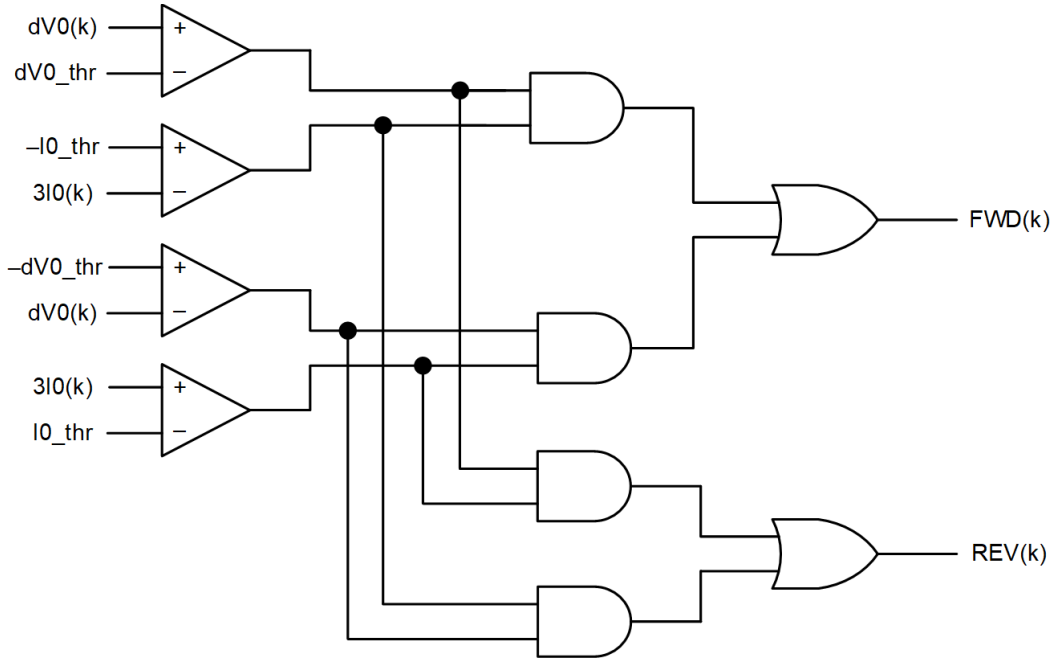


Fig. 8. Polarity check logic.

The forward counter logic is illustrated in Fig. 9. The reverse counter logic follows the same structure as the forward counter logic. The forward counter logic is executed only when the corresponding enable signal (FWD_EN) is active.

The logic for detecting the occurrence of an IGF is also shown in Fig. 9. This logic identifies a sudden change (or spike) in 3V0 by comparing the absolute value of the current dV0 to the maximum absolute dV0 observed over the most recent half to one cycle (max_dV0). If abs(dV0(k)) > 1.5 • max_dV0, the relay flag 3V0SPK is set for the duration of 3V0SPK_WIN. The same 3V0SPK logic applies to the reverse direction as well.

The 3V0SPK flag enables the FWD up-counter logic. This counter increments by one for each non-zero FWD set signal received from Fig. 8. If the counter output (cnts.fwd) remains non-zero and unchanged for three consecutive processing instances, the accumulated cnts.fwd value is cleared via the flag CNT_SAT.

If cnts.fwd exceeds a user-defined threshold (cnts_per_fwd_spike), the forward spike flag (FWDSPK) is set, indicating a forward directional IGF arc. Low-magnitude forward directional arcs are detected using the forward spike alarm flag (FWDALM), which is triggered when cnts.fwd exceeds another user-defined threshold (cnts_per_fwd_spike_alarm) and CNT_SAT is set. The FWDALM is set only if FWDSPK is not detected for that arcing event. Based on field events and real-time digital simulator (RTDS) simulations, we have found that setting cnts_per_fwd_spike equal to 3 and cnts_per_fwd_spike_alarm equal to 2 provides effective threshold values.

Based on field events, we have observed that, depending on the point on the wave at which restriking occurs during the voltage recovery period, the 3V0SPK signal may appear after one or two FWD counts. Since 3V0SPK is used to supervise FWD counting, this delay can cause the initial FWD counts to be missed. To enhance the dependability of forward IGF detection in such cases, we propose storing the FWD status immediately prior to the 3V0SPK event (i.e., FWD(k–1)) as a FWD_PRE flag. This flag can then be used in the cnt.fwd comparators to adjust the setting cnts_per_fwd_spike. For example, if the FWD_PRE flag is set, a FWD_Spike can be declared when cnts.fwd equals cnts_per_fwd_spike minus 1. Essentially, when the FWD_PRE flag is enabled, the parameter cnts_per_fwd_spike is decremented by 1. A similar approach can be applied to FWD_Spike_Alarms.

Upon detecting a forward directional spike, the forward counter logic is disabled for a user-configurable duration (block_fwd). This prevents a prolonged arc from being counted as multiple spikes and resets the counter logic, preparing it to accurately detect subsequent spikes.

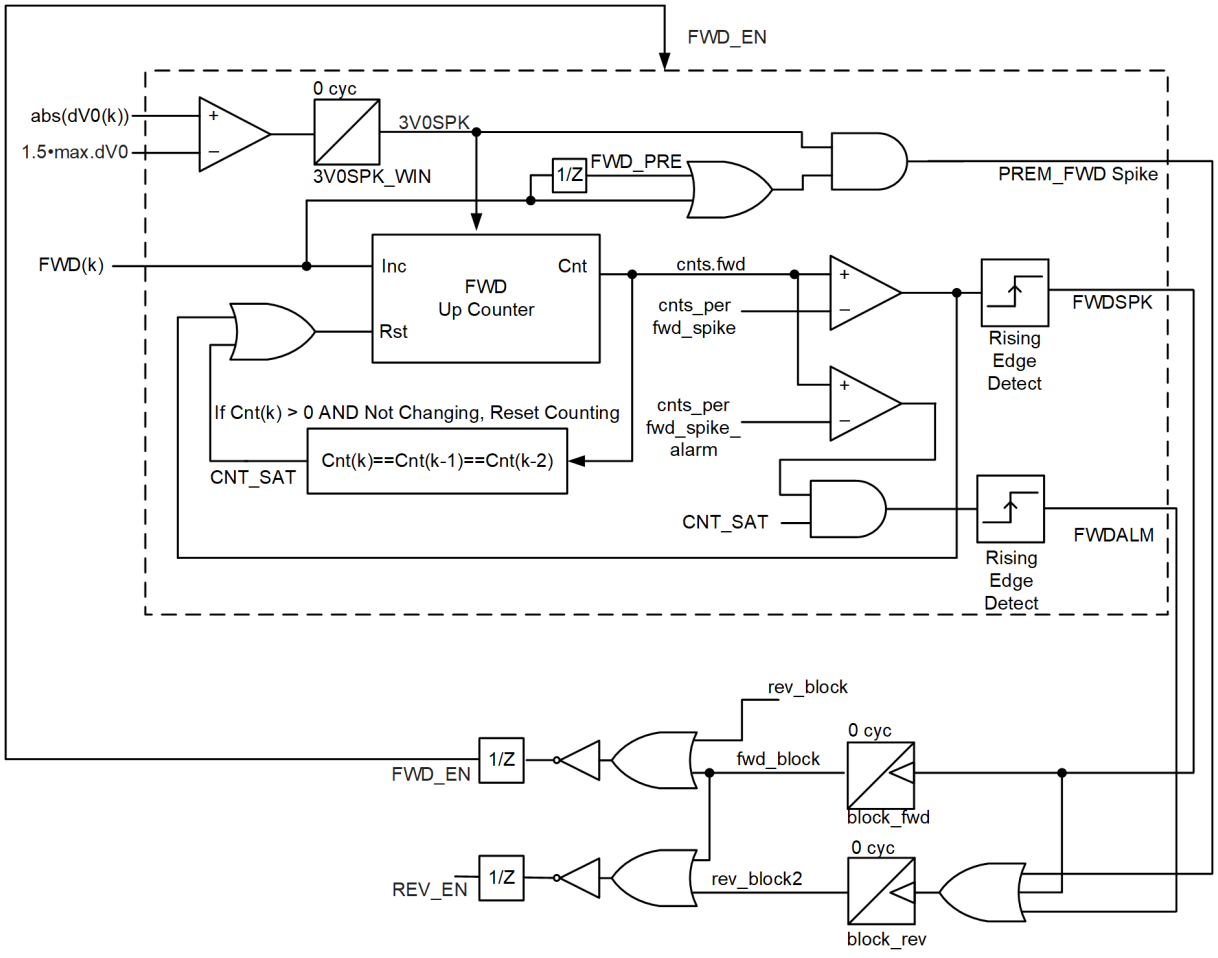


Fig. 9. Forward counter logic.

As explained earlier, since forward-clearing faults can appear as reverse faults, additional security is implemented to block the reverse counter logic. The reverse counter logic is disabled for an extended period; this is determined by the block_rev setting, under any of the following conditions:

1. A FWDSPK is detected
2. A FWDALM alarm is detected
3. A premature forward spike (PREM_FWD_Spike) is detected

The PREM_FWD_Spike flag is set if the FWD polarity flag is active just before the 3V0SPK flag is asserted or if the FWD flag is active during the 3V0SPK_WIN window. Field observations have shown that the spike in the 3V0 signal may be delayed, potentially missing the initial forward polarity check—especially if the arc is extremely short. To detect such short-duration arcing (faults that do not last long enough to trigger the FWDALM), the PREM_FWD_Spike mechanism is used. This enhances the security of the logic by blocking reverse counting in the presence of short forward arcs.

The FWD trip counter logic is shown in Fig. 10. We use a counting scheme to generate weighted fault counts. Each FWDSPK is assigned a weight of 1, and each FWDALM is assigned a weight of 0.5. We then accumulate the number of weighted FWDSPK and FWDALM counts over a user-defined period (FWDFLTWIN). If the total forward fault count (fwd_flt_cnt) exceeds the user-defined threshold (fwd_trip_cnt), then the FWDIGFTR bit is set. The IGFTR bit is set if FWDIGFTR or REVIGFTR is set where REVIGFTR is coming from the reverse logic. The logical setting reset_fwd_trip_counter can be used to reset the trip counter. For example, reset_fwd_trip_counter may be triggered upon detecting a fault other than an IGF through a relay trip equation. Although not shown in Fig. 10, similar counters could be implemented for the reverse logic. The IGFTR bit can be used to supervise traditional phasor-based directional elements, such as the wattmetric element or the incremental conductance element.

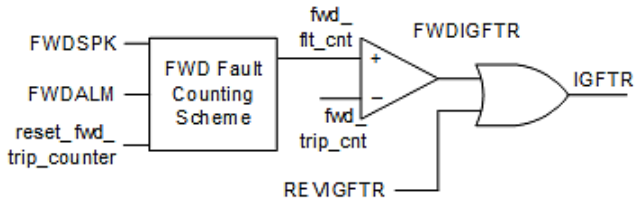


Fig. 10. Forward trip counter logic.

An IGF may develop into a persistent fault. Once a forward or reverse spike or alarm is detected, the persistent fault detection logic block can be executed to determine whether the fault is temporary or ongoing. This block uses 3V0 as its input. If the relay provides a fundamental-filtered output of 3V0 (or rms value), and the 3V0 magnitude does not decay over several cycles, the fault can be classified as persistent.

Alternatively, a peak detector can be applied to the 3V0 samples to identify the signal peaks. The current 3V0 peak is then compared to the previous peak. If the peaks are not decaying, or if the current peak is not less than a defined percentage (e.g., 5 percent) of the previous peak, a flag is set. If this flag remains true for a certain duration (a few cycles), then the persistent fault bit is asserted.

This persistent fault bit can enable traditional phasor-based directional elements, such as the wattmetric element or the incremental conductance element.

In certain installations of compensated grounded systems, REFCL technologies may be used alongside traditional Peterson coils to fully compensate the system during a single-phase-to-ground fault. This approach can reduce fault current to nearly zero, helping to mitigate wildfire risks or allowing loads to remain online for extended periods despite the presence of a fault. Although these systems respond quickly, they still require at least one power cycle to detect the fault and begin compensation [11].

Conventional phasor-based methods often struggle to detect permanent faults in these systems, as they typically require more than one power cycle to operate. In contrast, the proposed IGF directional method can detect arcing faults in less than a quarter of a power system cycle. As a result, equipment that injects current using inverters or compensates residual current by other means does not interfere with the proposed method.

The concept of combining FWD and REV spike detection with the persistent fault bit can be extended to identify ground faults and determine their direction in systems equipped with REFCL technology.

### *E. Approximate Petersen Coil Tuning*

This section presents a method to approximate percentage tuning of the Petersen coil. Understanding the percentage tuning is particularly valuable in systems with fixed or tapped reactor Petersen coil grounding, as the tuning level can vary with changing system conditions—such as the connection or disconnection of feeders or tap lines. The tuning approximation serves as a practical guide for operators, enabling them to adjust the taps and bring the system closer to 100 percent tuning, thereby enhancing overall performance.

The approximation can be done after a forward or reverse IGF spike. According to Fig. 4, the resonance frequency ($f_r$) of the compensated system during fault clearing is given by (3).

$$f_r = \frac{1}{2\pi\sqrt{3L_N(C_{0s} + C_{0L})}} \tag{3}$$

If the system is 100 percent tuned, the $f_r$ should be equal to the system nominal frequency ($f_n$ 50 Hz or 60 Hz). The $f_r$ can be approximated by a simple frequency measurement on the zero-sequence voltage using the zero-crossing method. Once the $f_r$ is known, the percentage tuning offset can be calculated as shown in (4).

$$tune_{offset} = \frac{f_r^2 - f_n^2}{f_r^2} \bullet 100\% \tag{4}$$

if $f_r > f_n$ (positive $tune\_offset$), then the Petersen coil reactance is less than the system capacitive reactance and the system is OC.

If $f_r < f_n$ (negative $tune\_offset$), then the Petersen coil reactance is more than the system capacitive reactance and the system is UC.

## VI. Results

The proposed logic was implemented in MATLAB and validated using real-world field events, and RTDS-simulated scenarios. All signals were sampled at a rate of 32 samples per cycle. The key parameters used in the MATLAB simulations are listed in Table I.

TABLE I
PARAMETERS USED IN THE IGF MATLAB MODEL

| Parameter | Value |
|---|---|
| 3V0_thr | 22 V (secondary) |
| dV0_thr | 1 V (secondary) |
| 3I0_thr | 1 mA (secondary) |
| cnts_per_fwd_spike | 3 |
| cnts_per_fwd_spike_alarm | 2 |
| cnts_per_rev_spike | 3 |
| cnts_per_rev_spike_alarm | 2 |
| block_fwd | 1 cycle |
| block_rev | 14 cycles |
| 3V0SPK_WIN | 0.25 cycle |
| fwd_trip_cnt/rev_trip_cnt | 5 |

We used an RTDS model to simulate phase-A-to-ground IGFs in an 11 kV, 50 Hz nominal system, as shown in Fig. 11. Since the fault resistance of IGF events is negligible, we limit the fault resistance to 20 mΩ. The Petersen coil has a fixed X/R ratio of 30. A damping resistor of 1,270 Ω is connected in parallel with the Petersen coil, supplying approximately 5 A during a solid ground fault. The per-phase line-to-ground capacitance is approximately 0.5 μF/km. Under normal operating conditions, with no loads connected, the total system capacitive current per phase is 39.2 A. Therefore, the 100 percent tuned inductance of the Petersen coil is 0.172 H.

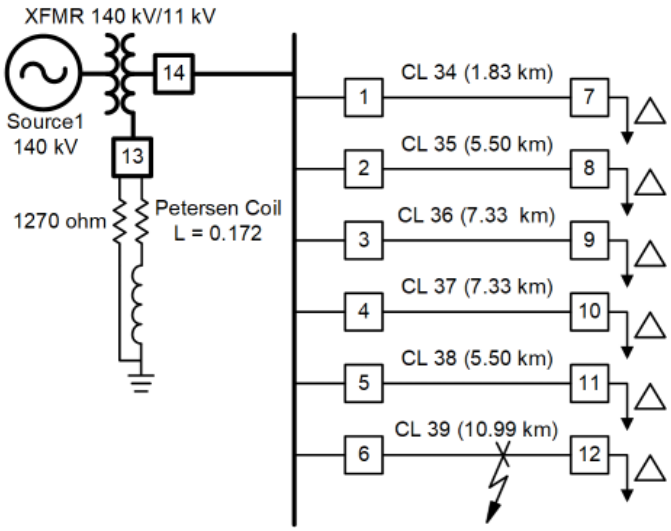


Fig. 11. Overview of the power system model developed in an RTDS.

### A. Simulated IGF Fault Detection Under Different Petersen Coil Tuning Conditions

This test was conducted to evaluate the effectiveness of the proposed method under different Petersen coil tuning conditions. Three system configurations were examined: a 100 percent tuned system, a 50 percent OC system, and a 50 percent UC system. The Petersen coil inductance values for each case are 0.172 H, 0.086 H, and 0.258 H. Forward IGFs were generated at the midpoint (50 percent) of the longest line (Line 39). Results are shown in Fig. 12, where Events 1, 2, and 3 represent the results for 50 percent UC, full (100 percent) tuning, and 50 percent OC, respectively.

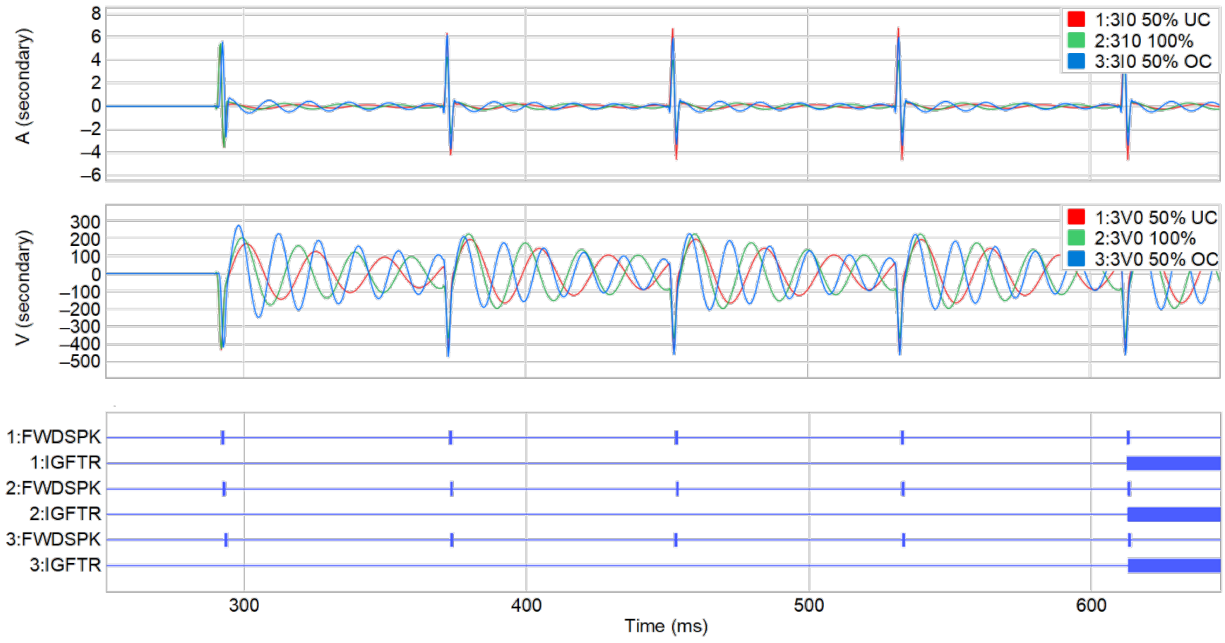


Fig. 12. Zero-sequence voltages, currents and IGF spikes detected by the proposed method under different Petersen coil tuning conditions (50 percent UC, full (100 percent) tuning, and 50 percent OC).

We observed that when the system is OC, both the zero-sequence voltage and the recovery voltage are at their highest. These values are lowest when the system is UC. As expected, the lowest zero-sequence current spikes occur when the system is fully compensated. Despite variations in Petersen coil tuning, the proposed method successfully detected all current spikes with the correct direction, and after reaching a forward fault count of 5 (fwd_flt_cnt = 5), the relay issued the IGFTR signal. Although not shown, we captured the reverse IGFs from the relay on the shortest line (Line 34), and the proposed method successfully identified their direction.

### *B. Simulated IGF Fault Detection With Different FLs*

This test was conducted to evaluate the effectiveness of the proposed method for different FLs along the feeder. Forward IGFs were generated in a fully tuned (100 percent tuned) system at 10 percent, 50 percent, and 90 percent of Line 39; the results are shown in Fig. 13. In Fig. 13, Events 1, 2, and 3 represent the results for 10 percent, 50 percent, and 90 percent FL.

In Petersen coil-grounded systems, the zero-sequence current and voltage are primarily determined by the system total capacitance and the coil tuning, rather than the FL. This is because the coil compensates for the entire network capacitive current, making the FL have minimal impact on system response. The system capacitance to ground is distributed throughout the network, so a fault at any point draws from this distributed capacitance. As a result, the total zero-sequence current remains nearly constant.

Therefore, the results show that the zero-sequence quantities do not vary significantly with the FL. The proposed method accurately detected the IGF spikes with the correct direction, and no variation was observed based on the FL. Also, after reaching a forward fault count of 5 (fwd_flt_cnt = 5), the relay issued the IGFTR signal.

Although not shown here, we also captured reverse IGFs from the relay on Line 34. The proposed method successfully identified their direction, again showing no dependence on the FL.

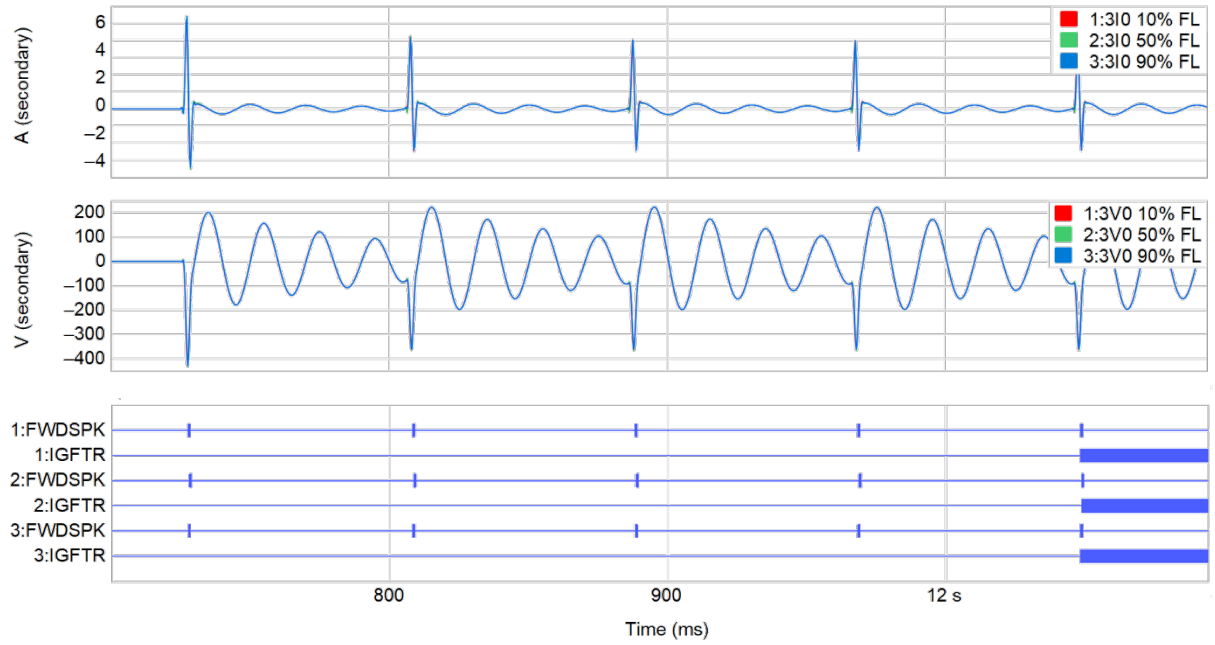


Fig. 13. Zero-sequence voltages, currents and IGF spikes detected by the proposed method with different FLs (10 percent, 50 percent, and 90 percent FL).

### C. *Simulated IGF Fault Detection With Different Feeder Lengths*

This test was conducted to assess the effectiveness of the proposed method with varying feeder lengths. The length of Line 39 was increased to 30 km. Forward IGFs were generated in a 100 percent tuned system at the 90 percent of both Line 34 and Line 39, and the results were compared. The new Petersen coil inductance was calculated as 0.115 H.

The forward IGFs on the shortest and longest feeders are shown in Fig. 14 and Fig. 15 respectively. In both figures, Event 1 corresponds to the shortest feeder (Line 34), which is 1.83 km long, while Event 2 corresponds to the longest feeder (Line 39), which is 30 km in length.

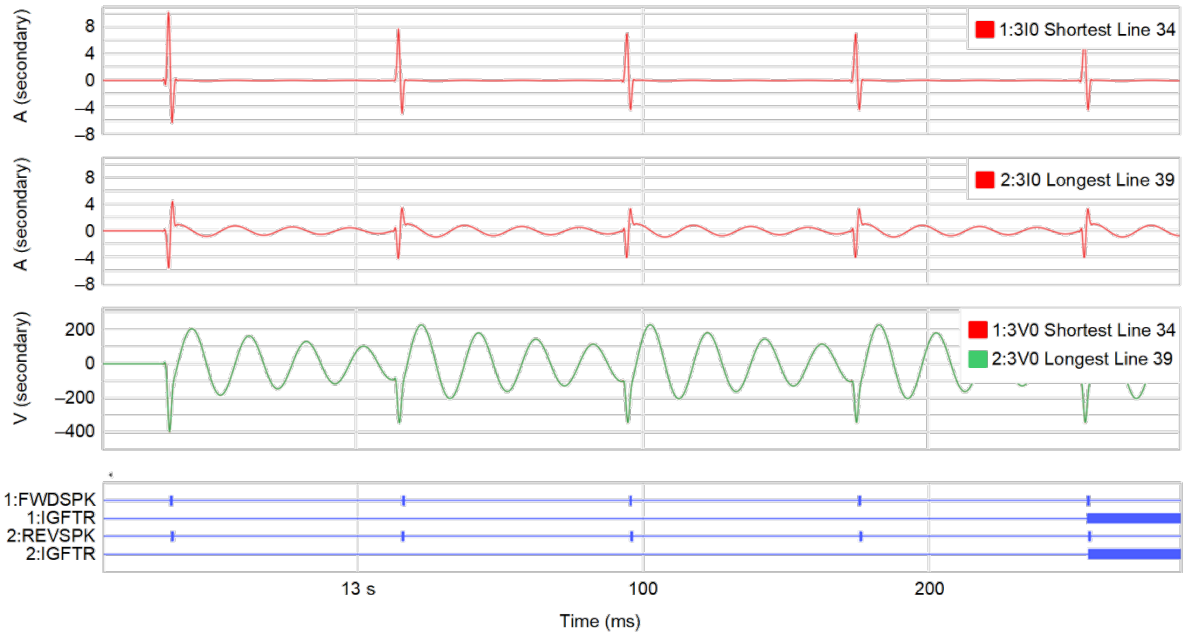


Fig. 14. Zero-sequence voltages, currents and IGF spikes detected by the proposed method with different feeder lengths for a forward fault on Line 34 (Event 1: Line 34, length 1.83 km, Event 2: Line 39, length 30 km).

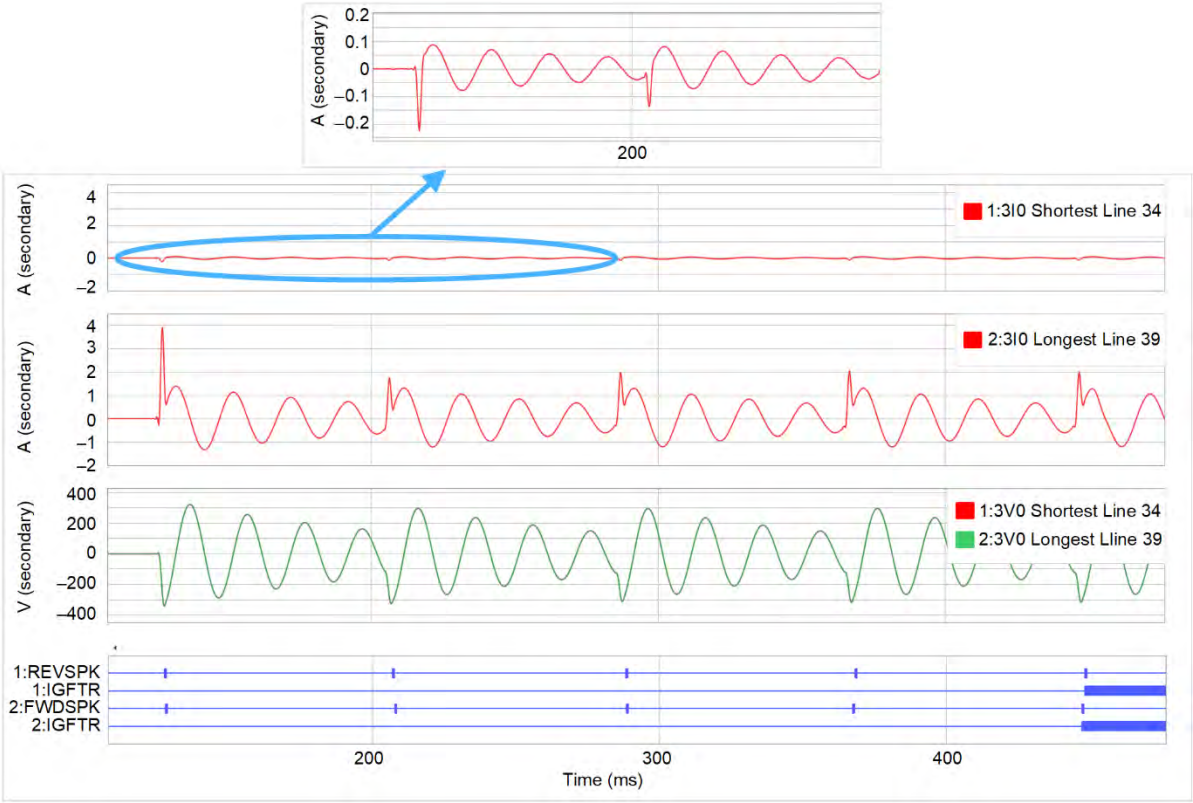


Fig. 15. Zero-sequence voltages, currents and IGF spikes detected by the proposed method with different feeder lengths for a forward fault on Line 39 (Event 1: Line 34, length 1.83 km, Event 2: Line 39, length 30 km).

According to (1) and (2), the zero-sequence current of a forward fault mainly depends on the distributed capacitance of the rest of the system, rather than the capacitance of the faulty feeder. In contrast, the zero-sequence current of a reverse fault on a feeder depends on the distributed capacitance of that feeder.

As a result, the highest forward zero-sequence current spikes are observed on the shortest line because the remainder of the system contributes the most capacitance in those cases. This behavior is illustrated on the 1:3I0 Shortest Line 34, shown in Fig. 14. Conversely, the smallest forward zero-sequence current spikes occur during forward IGF events on Line 39. This behavior is illustrated in the 2:3I0 Longest Line 39, shown in Fig. 15.

Comparing the 3V0s in Fig. 14 and Fig. 15, we can see that the transient peak of the zero-sequence voltage is higher when the zero-sequence current peak is higher. However, during the voltage recovery period, higher voltages are observed in the forward fault on Line 39. Due to this higher recovery voltage, the zero-sequence current on Line 39 during a forward fault recovery period can exceed that of the shorter line.

The magnitude of reverse IGF current spikes depends on the distributed capacitance of the feeder. Therefore, the longer the line is, the higher the peak of the current spike will be, as shown in Fig. 14 and Fig. 15. If the feeder is too short, detecting reverse IGF events can be challenging, as seen on the 1:3I0 Shortest Line 34, in Fig. 15.

Despite variations in feeder length, our proposed method successfully detects IGF spikes and correctly identifies their direction.

### *D. Simulated IGF Fault Detection With Different Fault Resistance*

This test was conducted to evaluate the effectiveness of our proposed method under different fault resistance conditions. Typically, the fault resistance in IGF events is negligible. In this study, we tested fault resistances of 20 Ω, and 500 Ω in a 100 percent tuned system. The results are presented in Fig. 16 where Event 1 and Event 2 illustrate 20 Ω, and 500 Ω results respectively.

The zero-sequence voltage is inversely proportional to the fault resistance, as shown in Fig. 16. As the fault resistance increases, the zero-sequence voltage decreases. Consequently, the zero-sequence current also decreases with increasing fault resistance, making IGF detection more challenging at higher resistance levels.

To improve sensitivity under these conditions, the threshold for 3V0_thr should be lowered. For a fault resistance of 20 Ω, a threshold of 22 V secondary was sufficient. However, for a fault resistance of 500 Ω, the threshold was reduced to 5 V. Field events have shown that the standing 3V0 is typically close to 0 V. Therefore, a 5 V threshold is considered secure for many applications, depending on the actual standing 3V0 level. In both cases, the proposed method successfully detected IGF spikes with the correct direction.

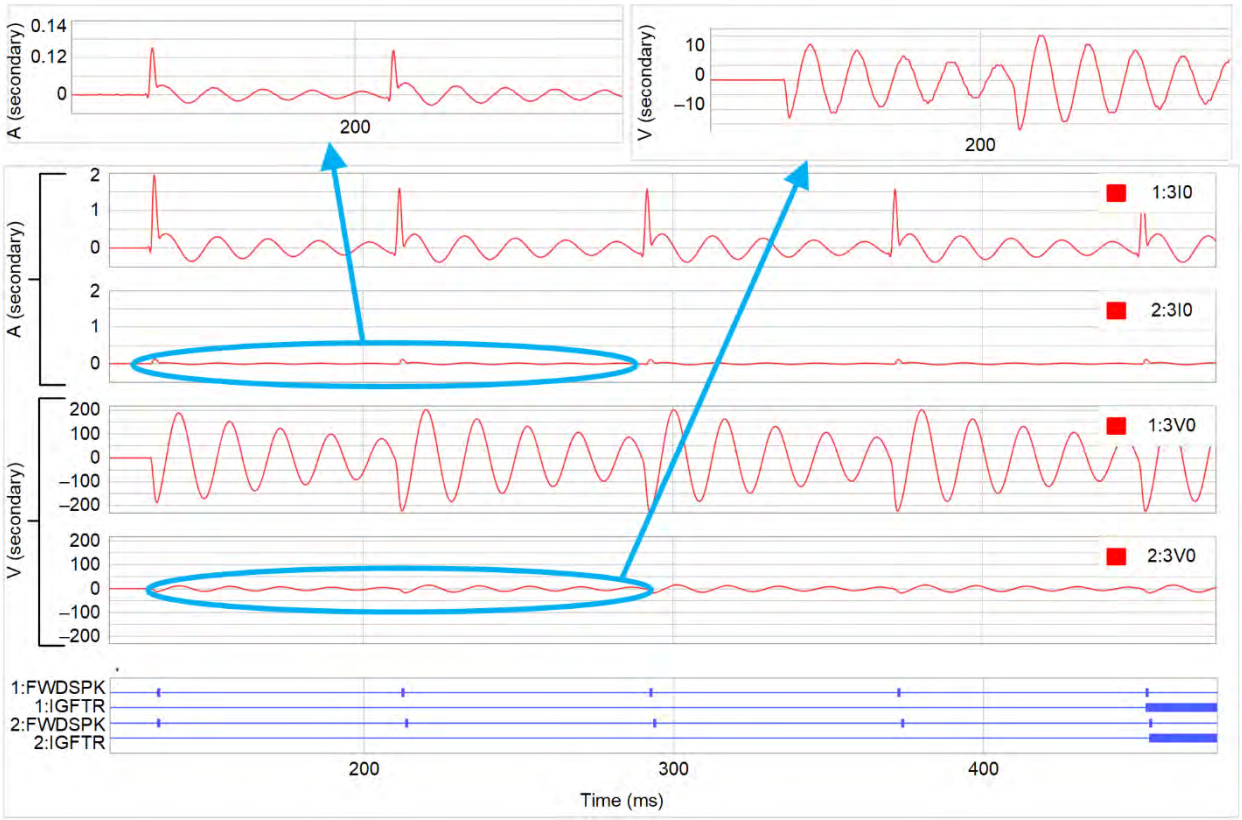


Fig. 16. Zero-sequence voltages, currents and forward IGF spikes detected by the proposed method with different fault resistances (Event 1: 20 Ω and Event 2: 500 Ω).

### *E. Real-World IGF Fault Detection Example 1*

Fig. 17 presents real-world IGF events captured by protective relays in a 10.7 kV, 50 Hz distribution system consisting of six feeders. During a solid ground fault, the system generated a total capacitive ground fault current of 118.58 A, while the Petersen coil supplied 118.67 A of actual compensation current. One specialty of this system is that one of the feeders (Bay 6) has a distributed compensation coil that contributes with 9.7 A. A damping resistor rated at 1,271 Ω is connected in parallel with the coil, contributing 4.86 A to the total active fault current, which is approximately 5.16 A.

The events were initially recorded at a sampling rate of 800 Hz and later resampled to 32 samples per cycle (1.6 kHz). Secondary values are shown in Fig. 17, with current and potential transformer ratios of 100 and 173, respectively.

Fig. 17 shows the zero-sequence voltage and current recorded by Relay 1 and Relay 2. We plotted two events on top of each other. Event 1 displays data from Relay 1, while Event 2 shows data from Relay 2. The IGF was in the forward direction relative to Relay 1 and in the reverse direction relative to Relay 2. This is evident from the observation that the 3I0 spikes were significantly larger in magnitude in Relay 1 compared to Relay 2. Since the zero-sequence voltage is common to both relays, their voltage waveforms are overlapped. A total of 12 forward spikes were recorded by Relay 1, and the proposed logic successfully identified all 12 with the correct direction. Similarly, the logic accurately detected all 12 reverse arcs recorded by Relay 2. After reaching a forward fault count of 5 (fwd_flt_cnt = 5), Relay 1 issued the IGFTR signal. Similarly, after reaching a reverse fault count of 5 (rev_flt_cnt = 5), Relay 2 issued the IGFTR signal.

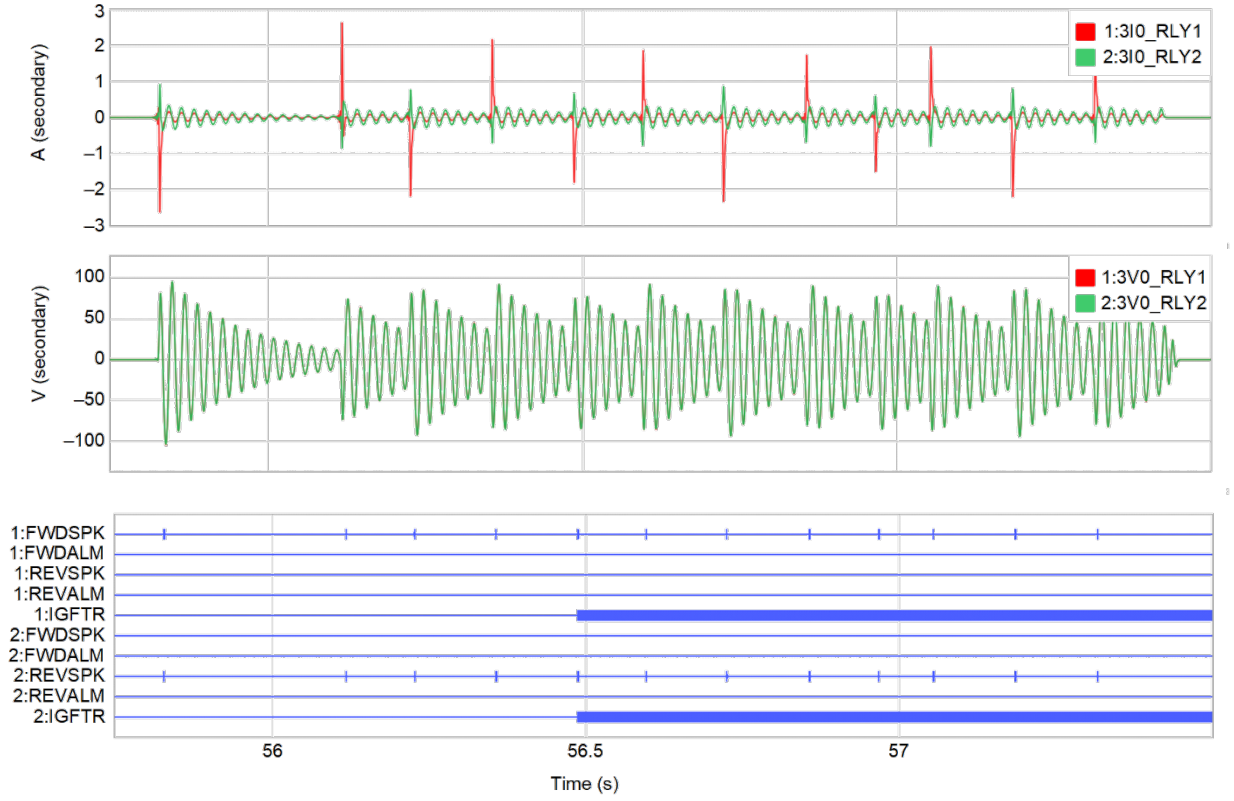


Fig. 17. Zero-sequence voltages, currents and IGF spikes detected by the proposed method in real-world example 1.

### F. Real-World IGF Fault Detection Example 2

Fig. 18 presents a real-world IGF event captured by a protective relay in a 10.7 kV, 50 Hz system. The system comprises seven feeders and is supplied by a 20 MVA, 140 kV/11.5 kV transformer. During a solid ground fault, the system generated a total capacitive ground fault current of 80 A. Of this, 70 A was compensated by a Petersen coil located at the substation, while an additional 10 A was supplied by a distributed Petersen coil. A damping resistor rated at 1,271 Ω was connected in parallel with the coil, contributing 4.86 A to the total active fault current, which was approximately 6 A.

The IGF is in the forward direction relative to the relay and develops into a permanent fault. The figure shows secondary values, with CT and PT ratios of 200 and 58, respectively. Out of a total of 11 spikes, the proposed logic successfully detected 5 forward spikes and 6 forward alarm spikes. After reaching a forward fault count of 5 (fwd_flt_cnt = 5), the IGFTR signal was issued. The assertion of the PERS bit indicates a persistent fault and can be used to enable any phasor-based directional logic.

### G. Petersen Coil Tuning Approximation

We used the same RTDS model shown in Fig. 11 to simulate short arc faults to validate the proposed tuning approximation. SLG arc faults were generated at 50 percent of Line 39. We tested three system conditions: a 100 percent tuned system, a 15 percent OC system, and a 20 percent UC system. We summarize system parameters and the expected values in Table II. We then compared the expected frequency during the voltage recovery period with the measured values from the RTDS simulation. The results for the tests are shown in Fig. 19, Fig. 20, and Fig. 21. The calculated $tune\_offset$ values from the simulation closely matched the expected values, as shown in Table II.

TABLE II
SYSTEM PARAMETERS AND RESULTS OF PETERSEN COIL TUNING APPROXIMATION

| System Tuning (Inductance) | Measured Resonance Frequency ($f_r$) | Calculated tune_offset |
|---|---|---|
| 100% (0.00% off tuned) (0.172 H) | 50.00 Hz | 0.00% |
| 15% over-tuned (0.145 H) | 54.24 Hz | +15.04% |
| 20% under-tuned (0.207 H) | 45.60 Hz | –20.19% |

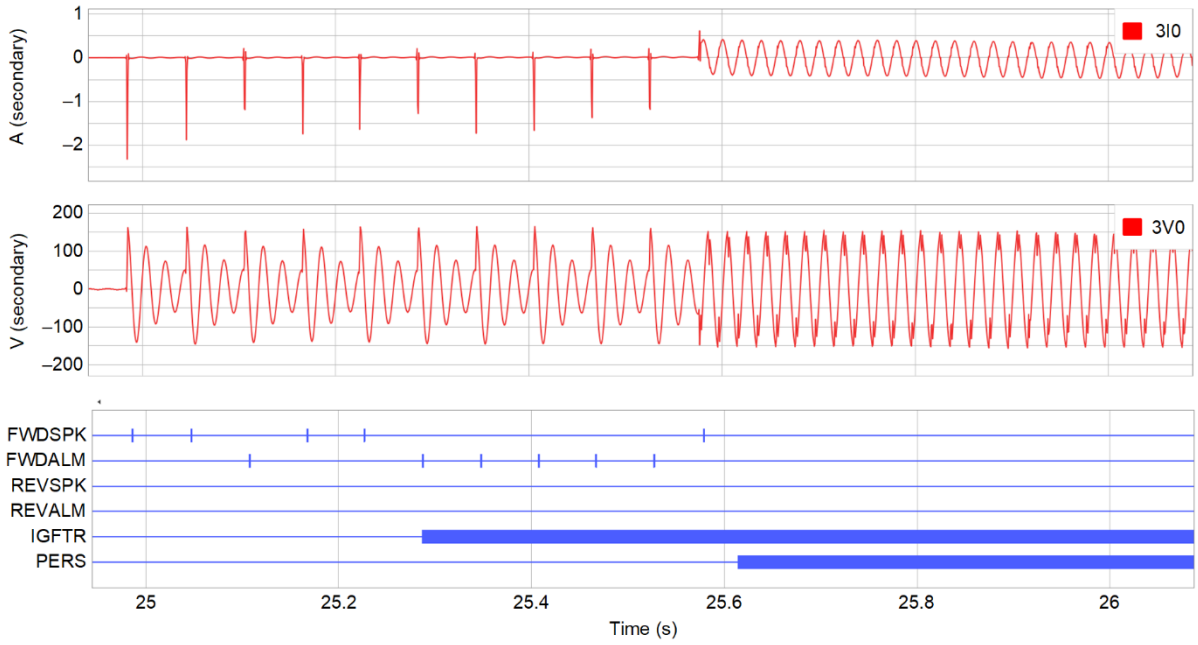


Fig. 18. Zero-sequence voltages, currents and IGF spikes detected by proposed method in real-world example 2.

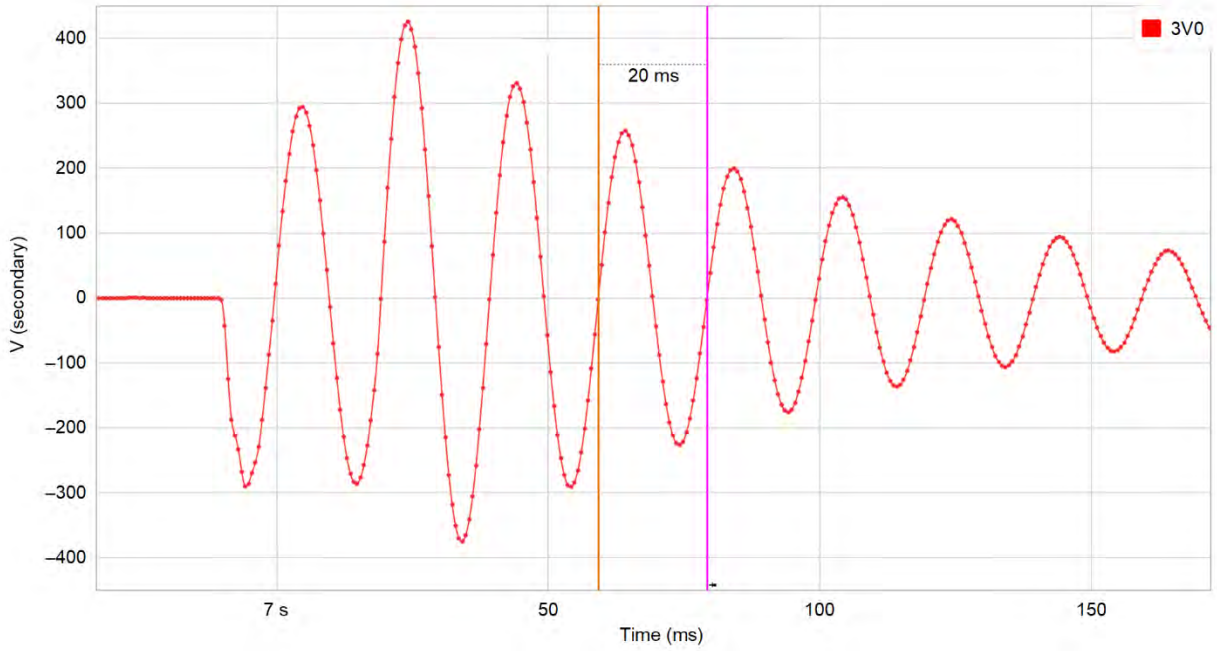


Fig. 19. In the 100 percent tuned system, measured resonance frequency is 50 Hz (nominal frequency).

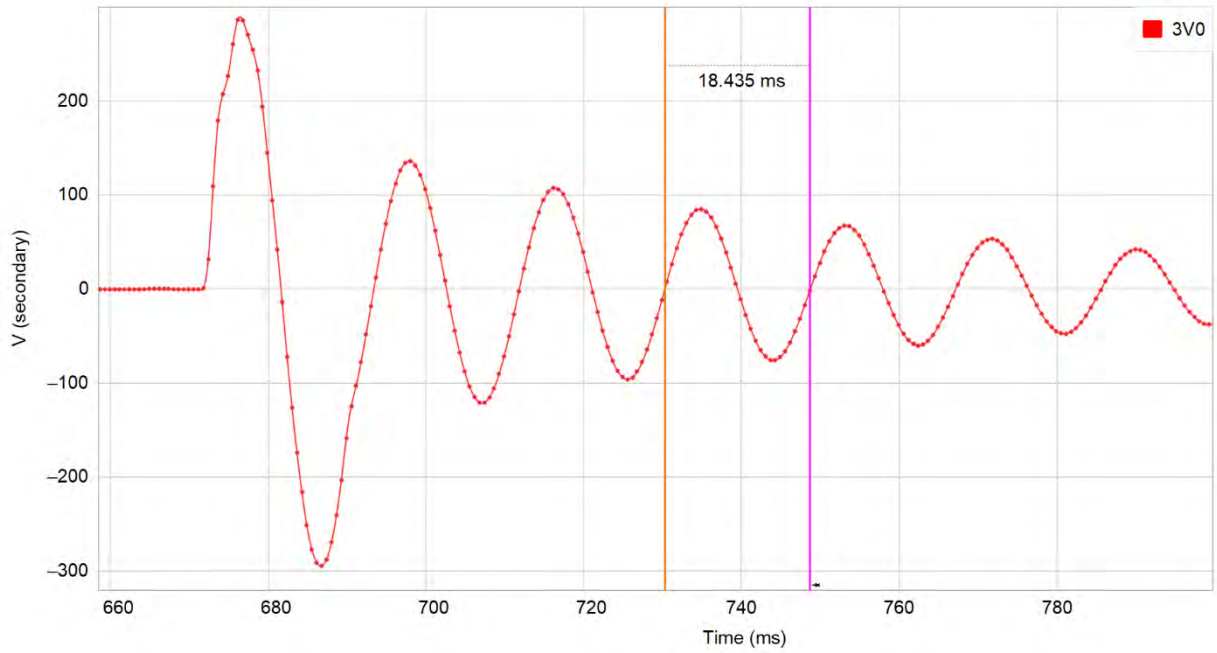


Fig. 20. In the 15 percent over-tuned system, measured 3V0 frequency is 54.24 Hz (higher than nominal frequency).

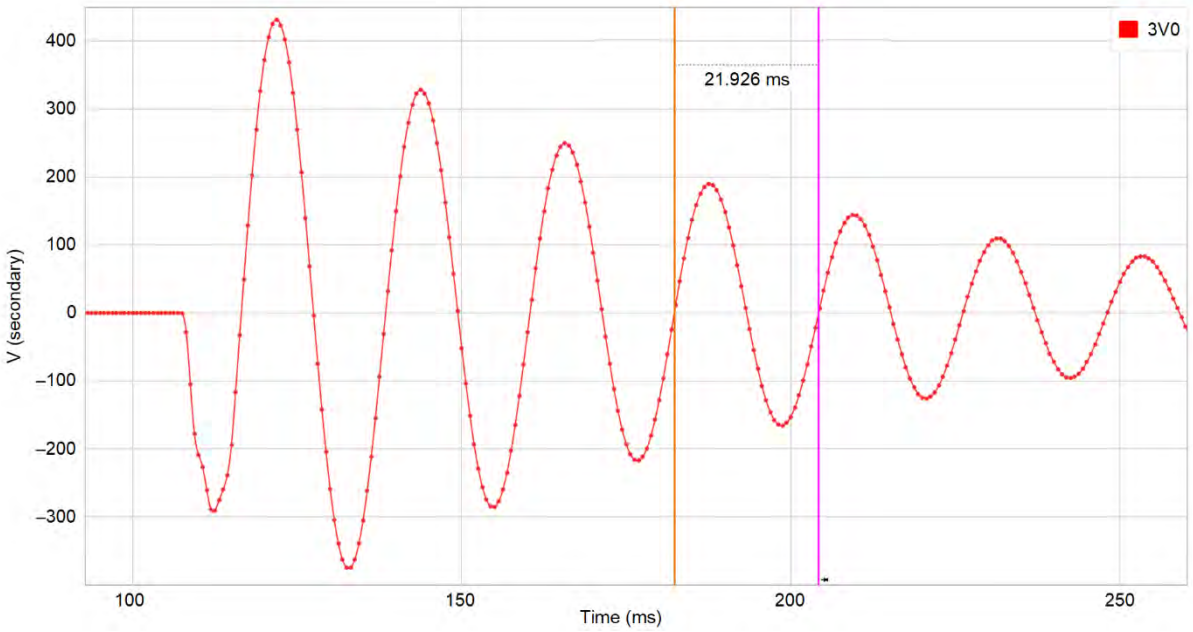


Fig. 21. In the 20 percent under-tuned system, measured 3V0 frequency is 45.6 Hz (lower than nominal frequency).

## VII. Conclusion

In this paper, we present a novel and practical method for detecting and determining the direction of IGFs in compensated grounded systems. Unlike traditional phasor-based or frequency-domain techniques, our proposed approach leverages raw zero-sequence current (3I0) and the change of zero-sequence voltage (dV0) to identify IGF events quickly and reliably. By comparing the polarity of dV0 and 3I0, our method effectively distinguishes between forward and reverse faults, even under challenging conditions, such as low fault energy, high fault resistance, or varying Petersen coil tuning.

The logic we propose is computationally efficient, requiring no complex transformations or high sampling rates, and is well-suited for implementation in digital relays. The simulation results presented in this paper, using RTDS and validated with real-world field data, demonstrate the robustness of our method across a wide range of system configurations, including different FLs, feeder lengths, and compensation levels. Additionally, this method can be used to enhance protection system security by blocking unreliable phasor-based directional elements during IGFs and to support persistent fault detection and Petersen coil tuning estimation.

Overall, our approach offers a significant advancement in the protection of compensated distribution networks, improving both dependability and security while maintaining simplicity and adaptability for modern protection systems.

## VIII. References

[1] J. Altonen, O. Mäkinen, K. Kauhaniemi, and K. Persson, "Intermittent Earth Faults-Need to Improve the Existing Feeder Earth Fault Protection Schemes,". *CIRED*, proceedings of the 17th International Conference on Electricity Distribution, Barcelona, Spain, May 2003, p. 6.

[2] A. Wahlroos and J. Altonen, "Application of Novel Multi-frequency Neutral Admittance Method Into Earth-Fault Protection in Compensated MV-Networks," proceedings of the 12th International Conference on Developments in Power System Protection, Copenhagen, Denmark, 2017.

[3] J. Berggren and L. Hammarson, "Novel Method for Selective Detection of Earth Faults in High Impedance Grounded Distribution Networks," CIRED, proceedings of the 18th International Conference and Exhibition on Electricity Distribution, Turin, Italy, 2005, pp. 1–4.

[4] "Arcteq Innovation: Intermittent Earth Fault Protection," *Arcteq,* Relayable Power, Finland, 2014. Available: arcteq.fi.

[5] T. Cui, X. Dong, Z. Bo, and A. Juszczyk, "Hilbert-Transform-Based Transient/Intermittent Earth Fault Detection in Noneffectively Grounded Distribution Systems," *IEEE Transactions on Power Delivery*, Vol. 26, Issue. 1, January 2011, pp. 143–151.

[6] M Lukowicz, W. Rebizant, and M. Kereit. "New Approach to Intermittent Earth Fault Detection with Admittance Criteria" *Elsevier International Journal of Electrical Power and Energy Systems*, Vol 123, December 2020.

[7] IEEE Std 142-1991, *Recommended Practice for Grounding of Industrial and Commercial Power Systems*.

[8] M. F. Abdel-Fattah and M. Lehtonen, "Transient-Based Protection As a Solution for Earth-Fault Detection in Unearthed and Compensated Neutral Medium Voltage Distribution Networks," Proceedings of the 2010 Electric Power Quality and Supply Reliability Conference, Kuressaare, Estonia, 2010, pp. 221–228.

[9] W. Zhengrong, C. Yingqian, T. Bing, X. Aidong, G. Xiaobin, and W. Gang, "Analysis of Overvoltage Caused By Intermittent Earth Fault and Its Suppression Method," *2016 China International Conference on Electricity Distribution (CICED)*, Xi'an, China, September 2016, pp. 1–5.

[10] Jeff Roberts, H Altuve, and D Hou, "Review of Ground Fault Protection Methods for Grounded, Ungrounded, and Compensated Distribution Systems," Schweitzer Engineering Laboratories, Inc., Pullman, WA, 2001.

[11] Y. Gong, G. P. Juvekar, N. Fischer, B. Glennon, J. Rorabaugh, J. Santillan, and A. Swisher, "A New Ground Fault Detection Method in Three-Wire Distribution Systems to Reduce Fire Hazards," proceedings of the 51st Annual Western Relay Conference, Spokane, WA, October 2024.

## IX. Biographies

**Henrik Sundholm** received his U.D. degree in electrical and electronics engineering from Chalmers University of Technology in Gothenburg Sweden in 1996. In 2015, he added courses from KTH Royal Institute of Technology in Stockholm, Sweden. He then began his career at the utility company Vattenfall Eldistribution, working at the Ringhals Nuclear Power Plant, as a protection application engineer. He later joined Birka Service, where he developed logic

for intermittent ground fault detection. He worked several years at Siemens AB as a senior application engineer and later for Siemens PTI as a power system consultant focusing on relay planning and protection coordination. He worked for the utility company Vattenfall Eldistribution, Stockholm specializing in protection planning and settings calculations. In 2022, he joined Proelektro as part owner and bord member, where he works as a senior power system engineer. His focus area is protection system coordination, planning, and power system protection and automation engineering for utilities and industrial plants.

**Anushka M. Dissanayake** received a BS degree in electrical and electronic engineering from the University of Peradeniya in Sri Lanka, in 2014. He went on to earn a Ph.D. degree in electrical engineering from Oklahoma State University in 2020. In 2020, he joined Schweitzer Engineering Laboratories, Inc. (SEL), where he is currently a lead power engineer in Research and Development. His research interests include power system protection, digital signal processing, and microgrids.

**Anirudhh Ravi** is a power engineer at Schweitzer Engineering Laboratories, Inc. (SEL). He earned his Bachelor of Technology (B. Tech.) degree in electrical and electronics engineering from SRM Institute of Science and Technology in Chennai, India in 2019. In 2021, he received his MS in electrical engineering from North Carolina State University at Raleigh. In 2022, Anirudhh joined SEL as an associate power engineer in Research and Development and is currently working as a power engineer.

**Osama Ansari** is a lead power engineer in Research and Development at Schweitzer Engineering Laboratories, Inc. (SEL). He joined SEL in 2021 as an application engineer in the Sales and Customer Service division focusing on power system protection and has since advanced to his current role. He previously worked as a protection engineer at Duke Energy Florida focusing on distribution protection coordination and settings calculations. He spent three years as a project and commissioning engineer in Mumbai, India, where he commissioned and tested MV/HV switchgears and transformers. He earned his bachelor's degree in electrical engineering from Sardar Patel College of Engineering, Mumbai, India, in 2014. Osama received his MS in electrical engineering from the University of South Florida in 2019, and an MS in cybersecurity operations and control management from Harrisburg University of Science and Technology in 2024. He is an active member of the IEEE.

**Vinod Yedidi** is a senior engineer in the Research and Development division of Schweitzer Engineering Laboratories, Inc. (SEL). He's been with SEL since 2006. Vinod received his MS in electrical engineering from University of Idaho in 2006 and his BS in electrical and electronics engineering from the Jawaharlal Nehru Technological University College of Engineering in Hyderabad, India, in 2002. He has been a member of IEEE for 25 years and is a registered professional engineer in Washington.

**Yusuf Zafer Korkmaz** received his B.Sc. in electrical and electronics engineering from the Middle East Technical University in Ankara, Turkey in 1995. He worked on protection and control schemes, substation automation and telemetry systems, and generator autosynchronization systems. In 2013, he joined Schweitzer Engineering Laboratories, Inc., where he works as a senior application engineer. His focus area is power system protection, automation, control, and communication systems for utilities and industrial plants. He is a member of IEEE.